HORM CANC (2011) 2:204–213
DOI 10.1007/s12672-011-0077-3

Novel Approaches to Quantify Estradiol-Induced Loss of ERβ1 Protein in Older Mouse Ovarian Surface Epithelium: New Tools to Assess the Role of ER Protein Subtypes in Predisposing to Ovarian Epithelial Cancer?

Linda S. M. Gulliver · Peter R. Hurst

Published online: 20 July 2011

Abstract Loss of estrogen receptor-beta (ERβ) occurs in ovarian epithelial cancer (OEC), a cancer of mainly older women. OEC is linked epidemiologically to hormone replacement therapy, predominantly with estrogen-only formulations. This study introduces a novel, non-biased method to quantify levels of estradiol-induced loss of ERβ1 protein, and defines, for the first time, normal OSE expression patterns for ERα and ERβ1 with advancing age. Older (7–10 months) Swiss Webster mice were injected with estradiol valerate (EV) while age-matched diestrous controls received oil. Mice were culled after 48 h, and blood and one ovary were frozen for estradiol RIA. Contralateral ovaries were paraffin-embedded for immunohistochemistry. Subsets of serial sections, triple-labeled with immunofluroescent tags, were imaged with confocal microscopy to provide optimal visualization of ER protein subtype expression in OSE. Immunofluorescence emission profiles distinct to ERβ1 in OSE were standardized and quantified in control mice then compared to profiles from EV-exposed mice. Estradiol levels were significantly elevated in EV-treated mice, both in blood ($p<0.0001$) and ovarian tissue ($p<0.001$), resulting in 11-fold reduction in OSE expression of ERβ1 protein ($p<0.0001$). In aging OSE, expression patterns of both ER subtypes varied within cells and with cell shape. ER co-localization appeared predominantly cytoplasmic and was infrequent in columnar compared to cuboidal-shaped OSE cells. Immunofluorescence emission profiling and multiple-label immunofluorescent tagging of ER using confocal microscopy, provides sharp definition of ER locus enabling concurrent qualitative and quantitative analysis of ER protein. It offers significant potential for assessing ER protein subtype status in predisposition to OEC.

Keywords Older mouse · Estrogen receptor · Quantitative immunofluorescence · Ovarian cancer

L. S. M. Gulliver (✉)
Faculty of Medicine, University of Otago,
Dunedin, New Zealand
e-mail: linda.gulliver@otago.ac.nz

P. R. Hurst
Department of Anatomy and Structural Biology,
Otago School of Medical Sciences, University of Otago,
Dunedin, New Zealand

Introduction

Epidemiological studies show increased risk for ovarian cancer in women over 50 years of age who have ever taken (or are current users of) hormonal therapy for perimenopausal symptoms, predominantly with use of estrogen-only formulations [1–8]. Recently, in an in vivo adult mouse model of ovarian cancer, exogenous estrogen was also shown to cause putative neoplastic change in normal OSE morphology and was linked to the earlier onset of OSE tumors and decreased animal survival time [9].

Estrogen's effects are mediated by estrogen receptor (ER), a member of the steroid hormone receptor superfamily [10], acting as a ligand-dependent transcription factor. ERα [11], initially thought to be the only functional ER, has been isolated in several species including mice [12]. A second functional ER, estrogen receptor-beta (ERβ), was subsequently cloned in rats [13], humans [14], and mice [15]. The sequence homology between ERβ and ERα in their DNA-binding domains is 96%, while the ligand-binding domain differs between the two receptors within the same species, sharing less than 60% sequence homology [16]. This likely

confers some of the diverse effects of activation of either receptor by the same ligand.

Kuiper and colleagues remarked on the high degree of variability in ERα and ERβ expression in different rodent tissues [13], suggesting that relative expression levels of ERα and ERβ, together with differences in their ligand-binding affinities, could contribute to estrogen's agonist/antagonist actions in any tissue type. It is well established that aside from ER homodimerization, co-expression of ERs both in vitro and in vivo can lead to heterodimerization of the two subtypes [17–20] and that in these partnerships, ERα dictates the functions of the heterodimer in genomic signaling pathways [20].

Both ERα, transcribed from the *ESR1* gene, and ERβ (*ESR2*) have variant transcripts in different species [16]. ERβ1 protein heterodimerizes with ERα, and as the only stand-alone functional ERβ [21], is the obligatory partner in the formation of in situ heterodimers with ERβ variants ERβ4 and β5. Both of these variants are proposed to enhance ERβ1 activity and are found in ovary. Relative expression patterns of ERα and of ERβ1 may therefore influence ovary-specific tissue responses to ER activation.

Targeted disruption of ERα [22] and ERβ [23] in female estrogen receptor knockout (ERKO) mice produces animals that survive to maturity and appear phenotypically indistinct from their wild-type counterparts. Mature female αERKO mice are however, infertile. Uteri are hypoplastic and enlarged ovaries are seen to contain hemorrhagic cysts with no preovulatory-sized follicles, and no corpora lutea. By contrast, βERKO mice are sub-fertile with decreased number and size of litters but have normal reproductive tracts with a hormonally responsive uterus (retained ERα expression). While ERKO-derived data serves to elucidate the role of ER in fertility, the role of ER in OSE aging and carcinogenesis remains poorly understood.

In ovarian epithelial cancer (OEC), ERβ1 has been named as a putative tumor suppressor [24], by virtue of mediating the proliferative influence of ERα on OSE [24], something also reported for breast cancer [25]. Down-regulation of ERβ mRNA is a reported feature of transition to oncogenesis involving OSE [24, 26, 27]. Levels of ER mRNA do not always correlate with functional protein however [26, 28, 29], perhaps restricting current knowledge of the role ER protein subtypes in OEC in vivo.

Mazouni and colleagues [30] recently used enzyme immunoassay (EIA) to quantify ER protein expression, citing the value of this method in predicting survival rates in breast cancer (and conceivably in determining patient responsiveness to adjuvant hormonal therapy). The authors also commented on the potential for quantitative immunohistochemical analysis of ER to obtain the same outcomes, however they did not develop a protocol to attempt this themselves.

To our knowledge, ERα and ERβ protein isoforms have not been quantified, nor their co-expression documented in normal and estrogen-exposed OSE from older subjects. This is surprising, given the vast majority of sporadic ovarian epithelial cancers occur in older mice [31, 32], rats [33], primates, domestic animals [34–36], and women [37]. In order to better understand ERβ's modulatory nature in OEC, a more advanced in vivo study of ERβ1 protein expression in OSE from older mice is desirable, since the hormonal profile of older subjects can differ appreciably from younger counterparts [38–42]. Indeed, paradoxically high endogenous serum estradiol concentrations have been reported for women during the perimenopausal transition that typically occurs in middle age [41–42].

Seven to 10 months of age is representative of middle age in mice, and the decline of hypothalamic–pituitary–ovarian hormonal function in middle-aged rodents has been reported to parallel that seen in women of middle age [38–40]. The present study therefore describes a novel, non-biased method, used to quantify ERβ1 protein expression in OSE from older estrogen-treated mice using multiple-label immunofluorescence and confocal microscopy. Normal expression and co-expression patterns for ERα and ERβ1 protein in aging OSE are also defined. We suggest quantitation of ER using this optimized IHC method may effectively be superior to EIA, since it would concurrently allow for the spatial study of ER expression and co-expression patterns within tissue compartments of interest.

Materials and Methods

Animals

Swiss Webster mice (7–10 month old) were group housed under standard conditions of 12-h light/dark cycle, with temperature and humidity control. Animals had pellet food and water ad libitum. Ethics approval was obtained (University of Otago Animal Ethics Committee). To establish whether mice had ovarian cycles, vaginal cytology was assessed daily for four consecutive estrous cycles. On day 0 of the experiment, animals were weighed and randomly assigned to two main treatment groups, (n= 8 mice—oil control group and 5 mice—estradiol valerate (EV)-treated group). Extra animals were included in the control group to ensure enough mice were in diestrous at sacrifice, since preliminary trials suggested high endogenous levels of estradiol led to decreased ER expression (in agreement with Hiroi and colleagues) [43]. Experimental animals received subcutaneous (SC) EV, 10 μ/g body weight in castor oil (CO), while controls had equivalent volumes of CO alone. Sacrifice was 48 h following injection. Two additional groups of four (diestrus) mice received either no

intervention (NI) or an SC injection of CO, and were sacrificed immediately to act as controls for the CO vehicle.

Blood and Tissue Collection

Mice were killed by ip injection of pentobarbitone sodium 60 mg/mL (0.1 mL) and blood withdrawn for estradiol assay. After overnight refrigeration at 4°C, blood was centrifuged at 1,500×*g* and serum stored at −20°C until assayed. One ovary was snap frozen in liquid nitrogen, and stored at −80°C for ovarian tissue estradiol assay. Uteri and oviduct were likewise obtained. Contralateral ovaries were fixed in 4% paraformaldehyde and paraffin-embedded for immunohistochemical analysis of ER.

Tissue Estradiol Extraction and Estradiol Radioimmunoassay

Estradiol extraction from thawed homogenized ovaries was overnight at 4°C using 70% methanol. Excess aqueous phase was removed by Centrivap Concentrator, (Uniscience), and residue frozen at −20°C prior to assay. To calculate extraction efficiency, 50 pg/mL of estradiol was added to extract derived from heart tissue, chosen for its absence of pericardial fat in mouse. Spiked and un-spiked heart tissue was assayed alongside ovarian tissue, producing an estradiol extraction efficiency of 86%.

RIA was with the DSL-39100 3rd Generation estradiol kit (Diagnostic Systems Laboratories Texas, USA) according to manufacturer's instructions. Standard curves were generated during trials to optimize dilution ratios for blood and ovarian tissue samples. In each case, diluent consisted of a zero standard lacking estradiol. Standards and controls were assayed in duplicate (triplicate where reagents permitted) with unknowns in duplicate. The minimum detection limit for the assay was 0.6 pg/mL. Analysis was with Assay Zap software (version 2.0 Biosoft; Cambridge, UK). Results are presented as mean±SEM. Statistical significance was by two-way ANOVA and Bonferroni post test or *t* test using GraphPad Prism 4, version 4.0c statistical software (GraphPad Prism Inc; San Diego, California). A 95% confidence interval was applied. $p<0.05$ was considered statistically significant.

Immunohistochemistry for ERα and ERβ1

A random set of numbers (GraphPad Software) was used to ensure a non-biased tissue sample from throughout each ovary. Serial sections were cut to either 5 μm for initial ER immunohistochemical localization using diaminobenzidine (DAB) and light microscopy, or 20 μm for immunofluorescent localization and quantitation of ER using a Zeiss Axioplan Upright Confocal microscope and LSM control software 510 (Windows NT); five sections/ovary, $n=5$ ovaries/group). Some thick 20 μm sections were also labeled with DAB and examined under the light microscope after it was noted in preliminary trials that visualization of ERβ was better as section thickness increased.

After de-waxing and rehydration through graded alcohols, sections were rinsed in double distilled water. Endogenous peroxidases were blocked with 3% (*v*/*v*) hydrogen peroxide in methanol/TBS. Antigen retrieval was by microwaving sections in 0.01 M citrate buffer (pH 6), for 10 min, and protein block by incubating sections with TBS/Triton and 0.25% BSA for 30 min at RT. Primary antibody incubation was overnight at 4°C using C1355, rabbit polyclonal (ERα; Upstate/Millipore, CA) diluted 1:100, or NCL-ER-beta, mouse monoclonal clone EMRO2 (ERβ; Novacastra, UK) diluted 1:50 in dilution buffer. Antibodies did not cross-react. Notably, the NCL-ER-beta antibody epitope mapped to a 17-amino acid region specific to the wild-type form of the C terminus of the receptor. This epitope is unique to ERβ1 and not present in spliced variant ERβ2 discovered in rodents by Chu et al. [44].

For light microscopy, sections were incubated for 60 min at RT with secondary antibody; biotin-conjugated donkey anti-rabbit IgG (Amersham Bioscience, UK), ERα, or biotin-conjugated goat anti-mouse IgG (Amersham), ERβ, diluted 1:200 in TBS. Signal amplification was with a 30-min incubation in a 1:100 dilution of streptavidin-biotinylated horseradish peroxidase reagent (Amersham) and sections were visualized with DAB (Fast DAB, Sigma). Gill's hematoxylin counterstained nuclei. Visualization of immunofluorescence required secondary antibodies diluted 1:200 in TBS directly conjugated to fluorochromes (ERα, Donkey anti-rabbit conjugated to Alexa Fluor 488, and ERβ, Donkey anti-mouse conjugated to Alexafluor 555; Molecular Probes, Inc. Eugene, Oregon). Sections were incubated for 2 h in the dark. Nuclear counterstaining was with TO-PRO-3 (T3605 monomeric cyanine nucleic acid stain; Invitrogen, USA) 1:1,000 in TBS. Positive controls included uterus (ERα) and oviduct and skin (ERβ). Three negative controls were included. The first omitted primary antibody, the second consisted of a non-immune IgG control diluted 1:100 (α) or 1:50 (β) in dilution buffer, and the third consisted of tissue from ERKO mice lacking the receptor for ERα (skeletal muscle) or ERβ (testis), respectively.

Quantitative Analysis of ERβ1

Specimens were located with the 4× objective lens of the confocal microscope using low transmitted light. Three areas of OSE were allocated for scanning using random numbers between 1 and 360, and a 360° transparent "clock" positioned over the projected image. Allocated areas were re-located, viewed at high magnification using the 63× objective lens and oil immersion, and the light source

changed to laser (excitation wavelengths 543 or 488). The area of interest was twice further magnified using the zoom function of the microscope software. Settings were briefly calibrated to produce best signal-to-noise ratio by adjusting the detector gain (DG) of the LSM software, and using an optical slice thickness of <2 μm. The minimum possible laser intensity to obtain images was held constant throughout scans. Software configurations were recorded for sections viewed, and DG settings averaged for control specimens during individual scanning sessions. Averaged DG settings from control OSE were used to generate baseline DG configurations for scans of EV-exposed OSE and were similarly used to determine fluorescence emission from negative (IgG or no primary) controls. DG configurations from control ovaries scanned across multiple sessions were compared to ensure no significant difference existed.

Captured images were stored for measurement of immunofluorescence emission. Using Image J software, a central line was drawn through a 50-μm length of OSE, producing distinct ERβ1 immunofluorescence profiles for each scan. As the line intersected ERβ fluorescent signal, the signal was transduced and given a numerical value (Fig. 4 represented on the *y*-axis). OSE length was projected along the *x*-axis. Fluorescence intensity scores were averaged for control and treated groups, and statistical analysis performed (Mann–Whitney statistical test, GraphPad Prism 4, version 4.0c statistical software, GraphPad Prism Inc; San Diego, California). $p<0.05$ was considered statistically significant.

Results

Estradiol Radioimmunoassay

There were no significant differences between NI and CO mice in serum or ovarian tissue estradiol concentration. EV-treated mice showed significantly elevated serum estradiol levels (1,382±138 pg/mL, 95% CI, 1,028–1,736 pg/mL) compared to controls (37.8±12.5 pg/mL, 95% CI, 2.9–72.3 pg/mL), $p<0.0001$. Ovarian tissue estradiol concentration was 11 times higher in EV-treated animals (760±139 pg/mg tissue, 95% CI, 418.2–1,102.0 pg/mg), compared to controls 66.2±7.5 pg/mg, 95% CI, 47.8–84.6), $p<0.001$. Inter-assay variation coefficients were 8.02% (serum) and 8.57% (ovary). Intra-assay variation coefficients were 3.2% (serum) and 10.3% (ovary).

ERα and ERβ1 Protein Expression in Older Normal and EV-Treated OSE

Immunohistochemistry (Light Microscopy)

Figure 1 shows typical ER expression patterns in OSE from control and EV-treated mice using DAB and light microscopy. Tissue from mice lacking the gene for ERα (αERKO, skeletal muscle) and ERβ (βERKO, testis) was included as additional negative controls. Both ERs are present in skeletal muscle cell nuclei, and adult mouse testicular interstitial cells from wild-type mice, with ERβ additionally found in Sertoli and sperm cells [45, 46]. Images represent the results of 4 repeated immunohistochemical experiments.

ERα Expression

In control mice, strong levels of ERα staining were seen in OSE, and also in underlying stromal fibroblasts and interstitial cells (Fig. 1a). Qualitatively, ERα expression appeared reduced in both OSE and stroma of EV-treated animals (Fig. 1b).

ERβ1 Expression

ERβ displayed particulate staining and was abundantly expressed in control OSE from diestrus mice (Fig. 1f). Interestingly, ERβ1 could be just visualized in 5 μm sections, but was far more apparent in the thicker sections (Fig. 1f*). Unlike ERα, ERβ expression in underlying stroma from controls was minimal. Estradiol-treated mice had low, often non-detectable levels of ERβ in OSE overlying corpora lutea and preovulatory follicles where squamous or cuboidal-shaped cells dominated surface epithelium (Fig. 1g), yet high expression remained in OSE near OSE/mesothelial boundaries, and in areas of cell layering and invagination where OSE cells were columnar in shape. Overall, qualitative analysis at light microscopy level indicated a very large downregulation of ERβ in estradiol-exposed OSE.

High-Resolution Immunofluorescent Localization of ER (Confocal Microscopy)

Figure 2 shows confocal images representative of OSE from four diestrus controls.

Triple label immunofluorescence (Fig. 2a–j) yielded high-resolution images that defined expression patterns for both ER subtypes. ERα was the dominant isoform but expression varied with cell shape. Columnar OSE cells (Fig. 2f–j) had a more diffuse fluorescent label for ERα. Single immunofluorescent label for ERβ (Fig. 2b, g) indicated this receptor formed discrete clusters, accounting for the particulate staining pattern observed by light microscopy. Cluster size also varied with cell shape with large clusters frequently observed in columnar OSE (Fig. 2g). The nuclear stain TO-PRO-3 confirmed nuclear location of ERα and ERβ (Fig. 2d, e, i, j). However, both ER also localized to the cytoplasm, with co-localization appearing to be mainly cytoplasmic. Nuclear ERβ clusters

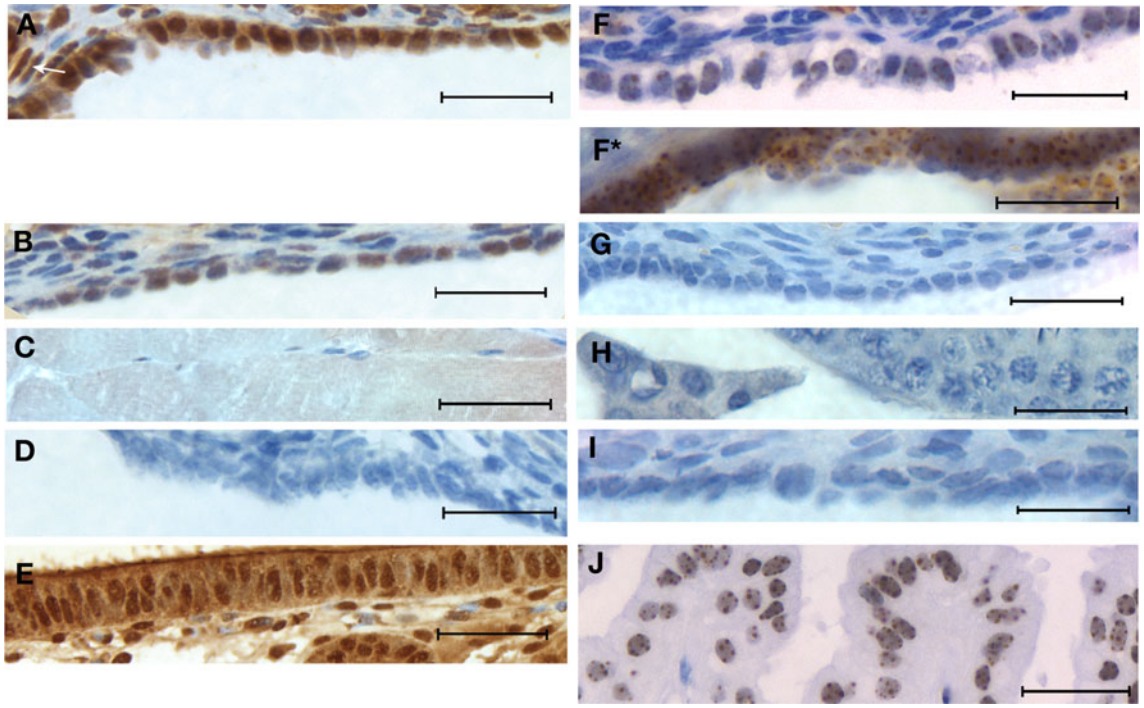

Fig. 1 Immunohistochemical localization of ER in OSE with light microscopy and DAB. **a** Control ovary showing high ERα expression in OSE and in underlying stromal fibroblast (*arrowed*) and interstitial cells. *Scale bar*=25 μm. **b** EV-treated ovary showing reduced expression of ERα in both stroma and OSE. *Scale bar*=25 μm. **c** Negative control (1) ER alpha knockout (αERKO) mouse skeletal muscle showing no immunoreactivity in nuclei (*blue*). *Scale bar*=30 μm. **d** Negative control (2) primary antibody replaced with IgG isotype serum showing no immunoreactivity. *Scale bar*=25 μm. **e** Positive control for ERα (uterine epithelium of estrus mouse) showing strong nuclear and cytoplasmic stain. *Scale bar*=50 μm. **f** Ovary section (5 μm) from control mouse showing the characteristic particulate distribution of ERβ1 in OSE (optimally visualized in OSE cells as section thickness increased to 20 μm (*F**). *Scale bars*=25 μm. **g** EV-treated ovary showing absence of ERβ1 receptor expression in OSE cells overlying a large follicle. *Scale bar*=25 μm. **h** Negative control (1) ER beta knockout (βERKO) mouse testis tissue showing no immunoreactivity in either interstitial or germ cells. *Scale bar*=25 μm. **i** Negative control (2) primary antibody replaced with IgG isotype serum showing no immunoreactivity. *Scale bar*=18 μm. **j** Positive control. Oviduct (diestrus mouse) showing extensive particulate ERβ1 immunoreactivity. *Scale bar*=25 μm

predominantly corresponded to sites of nuclear heterochromatin. Although not quantified, co-localization of ERα with ERβ appeared more frequent in cuboidal-shaped OSE. ERβ1 expression was also observed to be greater in columnar-shaped OSE.

Analysis of dual immunofluorescence profiles (Fig. 3a–j) showed the two receptors generally localized close to each other in OSE cells.

Quantitation of ERβ1 Protein Expression in Older OSE

Single label immunofluorescence profiles generated by ERβ1 from control OSE frequently produced fluorescence emission spikes of between 200 and 250 arbitrary units (Fig. 4a). In contrast, immunofluorescent profiles from EV-treated mice showed a very large reduction in fluorescence emission (Fig. 4b). Fluorescence intensity scores averaged across all OSE scans confirmed 11-fold reduction in ERβ1 expression ($p<0.0001$, Fig. 4d). Figure 4c shows replacement of primary antibody with an IgG isotype serum resulting in no detectable fluorescent signal.

Discussion

Using a novel combined immunofluorescent–confocal approach, this study was able to demonstrate that receptor levels of ERβ1 protein decline 11-fold relative to diestrous controls within 48 h of exogenous estradiol exposure. Moreover, we were able to show that this large reduction in ERβ1 expression was in response to not only significantly elevated serum levels of estradiol, but also ovarian tissue levels. This raises the possibility that exogenous estradiol may become sequestered into ovarian tissue, causing downregulation of ERβ1 protein and altering normal expression patterns for ERβ1 relative to ERα. This could potentially impact on the tendency for older OSE to undergo neoplasia.

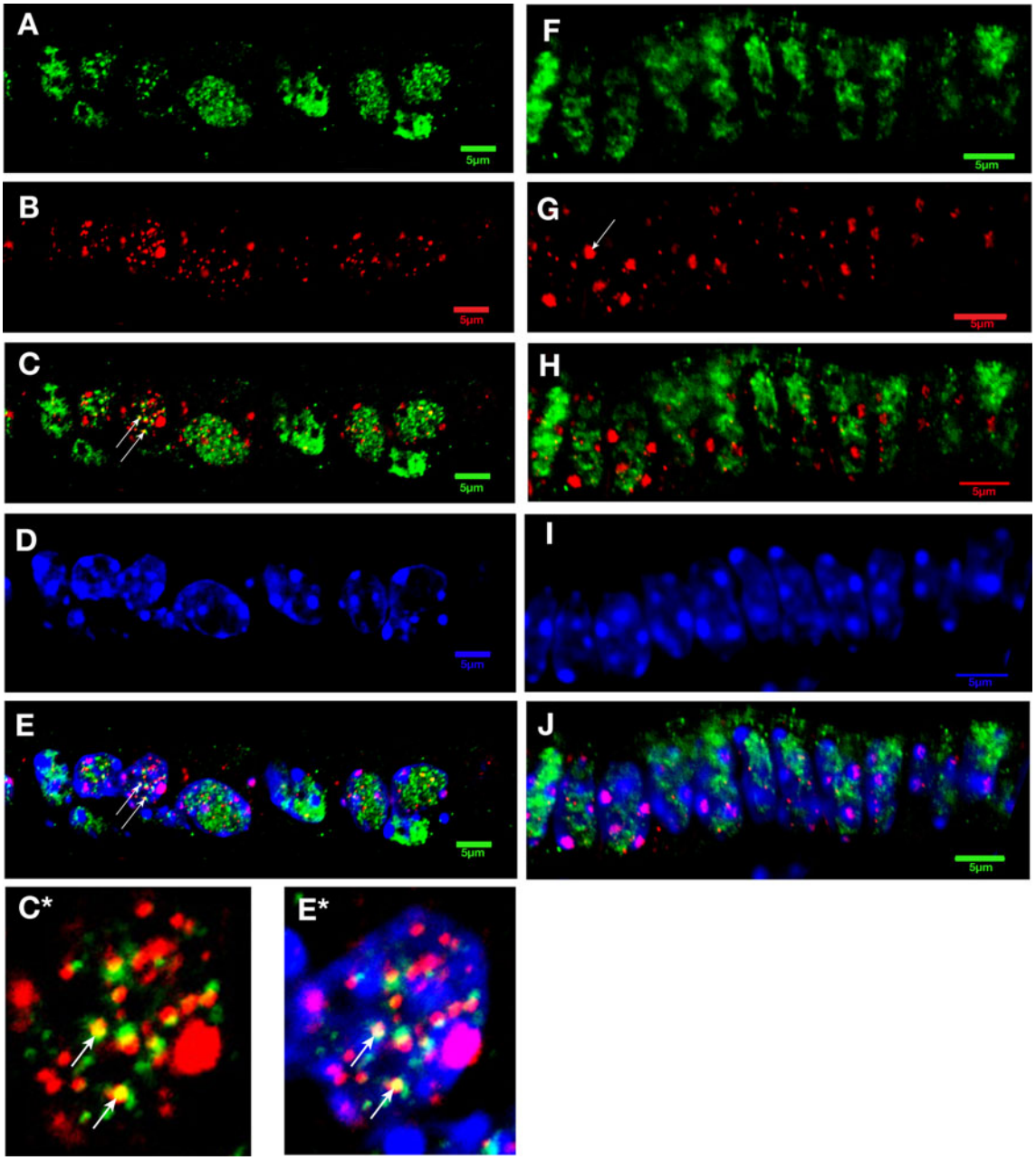

Fig. 2 Single, dual, and triple immunofluorescent localization of ER in OSE with confocal microscopy. Figures **a**–**e** show the same cuboidal and **f**–**j** the same columnar-shaped OSE cells. *Scale bars*= 5 μm. **a** ERα expression (*bright green*) in cuboidal OSE. **b** Single label for ERβ (*red*) shows that in cuboidal-shaped OSE, ERβ forms variable sized clusters. **c** Dual label for ERα (*green*) and ERβ (*red*). Areas where the receptors co-localize are yellow (*arrowed*) and can be viewed at high magnification (*C**). **d** Nuclei labeled with TO-PRO-3 (*blue*). **e** Triple immunofluorescent label. ERα localizes predominantly to nuclei green/aqua, but is also seen in cytoplasm (*bright green*). ERβ localizes to nuclei (*pink*) and there is some evidence for its presence in the cytoplasm (*red*). Areas of ERα/β co-localization appear predominantly cytoplasmic (*bright yellow arrowed* right side of image), but also occur amongst nuclear ER clusters (*pale yellow*/*white*, *arrows* left side of image). Image may be viewed at high magnification (*E**). **f** Columnar-shaped OSE cells show a more diffuse pattern of ERα expression (*bright green*) compared to cuboidal-shaped cells. **g** Large ERβ clusters (*arrowed*) are seen more frequently in columnar OSE than in cuboidal OSE. **h** Dual label for ERα and ERβ. Co-localization of ERα with ERβ is infrequent in columnar OSE. **i** Nuclei stained with TO-PRO-3. **j** Triple label immunofluorescence in columnar OSE shows ERα to be expressed mainly in the nucleus (*green*/*aqua*) although areas are seen where ERα localizes to the cytoplasm (*bright green*), producing a wispy appearance superior to the nuclear boundaries. ERβ clusters localize almost entirely to the nucleus (*pink*), but isolated smaller clusters are seen in the cytoplasm (*red*). Note that nuclear ERβ clusters usually correspond with heterochromatin regions

At light microscopy level, the present study additionally showed a decrease in ERα expression in OSE following estradiol, however downregulation of this isoform appeared to occur to a lesser degree than that of ERβ1. Given the

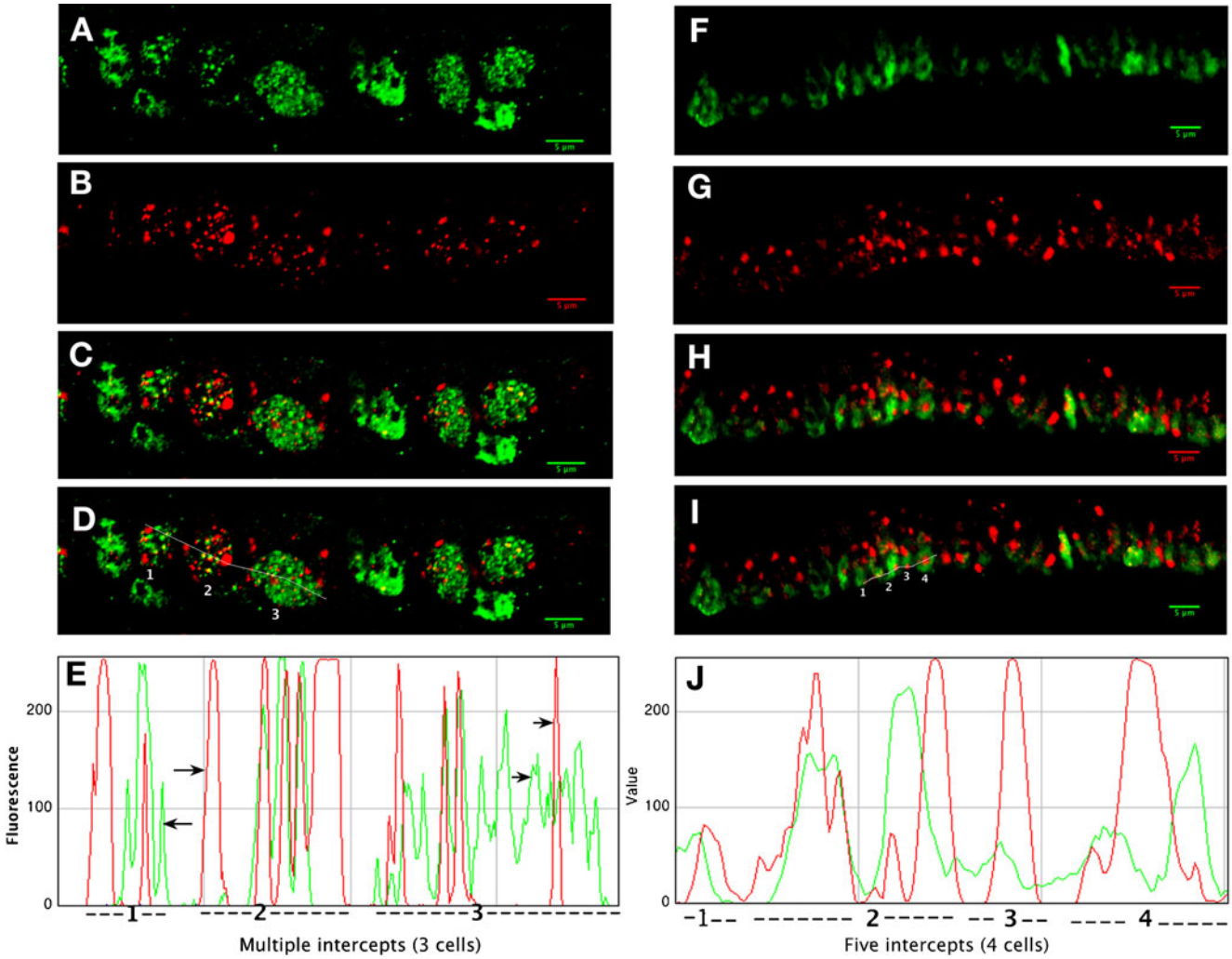

Fig. 3 Dual label immunofluorescent profiling in OSE showing the relationship of ERα to ER β. **a**, **b** Fluorescent label is shown for ERα (*green*), and ERβ1 (*red*) in cuboidal OSE. **c** Merged image of **a** and **b**. **d** Merged image shown in **c** where a line, drawn through a selection of three OSE cells (numbered), gives rise to multiple small intercepts where ERα and ERβ1 are detected in the same plane relative to the *z*-axis. Intercepts from the second OSE cell show areas of yellow fluorescence, indicating a shared receptor locus. Cells *1*, *2*, and 3 also show areas of distinct red fluorescence for ERβ1 and green fluorescence for ERα, indicating a close, but not a shared, receptor locus. **e** Immunofluorescence profile shows fluorescence emission for ERα (*green*) and ERβ1 (*red*) in the three probed OSE cells. Maximum fluorescence intensity produced by both ER overlaps in three out of five intercepts from cell *2*, confirming a shared receptor locus. Intercepts from cells 1 and 3 additionally show separations in peak fluorescence intensity (*arrowed*) denoting areas within these cells where ERα and ERβ1 do not co-localize. **f** ERα (*green*) in columnar-shaped OSE cells. **g** Particulate distribution of ERβ1 (*red*) in columnar OSE cells. **h** Merged fluorescence image of **f** and **g**. **i** Merged image (**h**) where a line drawn through a selection of four columnar OSE cells (numbered), gives rise to five intercepts where ERα and ERβ1 are detected in the same plane relative to the *z*-axis. **j** Immunofluorescence profile shows fluorescence emission for ERα (*green*) and ERβ1 (*red*) in probed columnar OSE cells. Maximum fluorescence intensity overlaps in intercepts 1 and 2. Intercepts 4 and 5 (cells 3 and 4) show gaps in peak fluorescence intensity, indicating a greater level of separation between the two receptors

relative insensitivity of light microscopic semiquantitative analysis of ER, it would now be desirable to use immunofluorescent profiling and confocal microscopy to quantify the extent of downregulation of one isoform relative to the other.

Although quantitative analysis of ER protein has previously been performed using Western blot and following enzyme immunoassay (EIA; [30]), the advantage of multiple-label immunofluorescence profiling over Western blot and EIA is that it allows for concurrent morphologic, morphometric and quantitative analysis of receptor isoforms co-expressed in the same tissue. Furthermore, since measurement of ER at mRNA level does not always correlate with immunoreactive protein [26, 29, 47], robust quantitative analysis of ER protein may be of significant clinical importance.

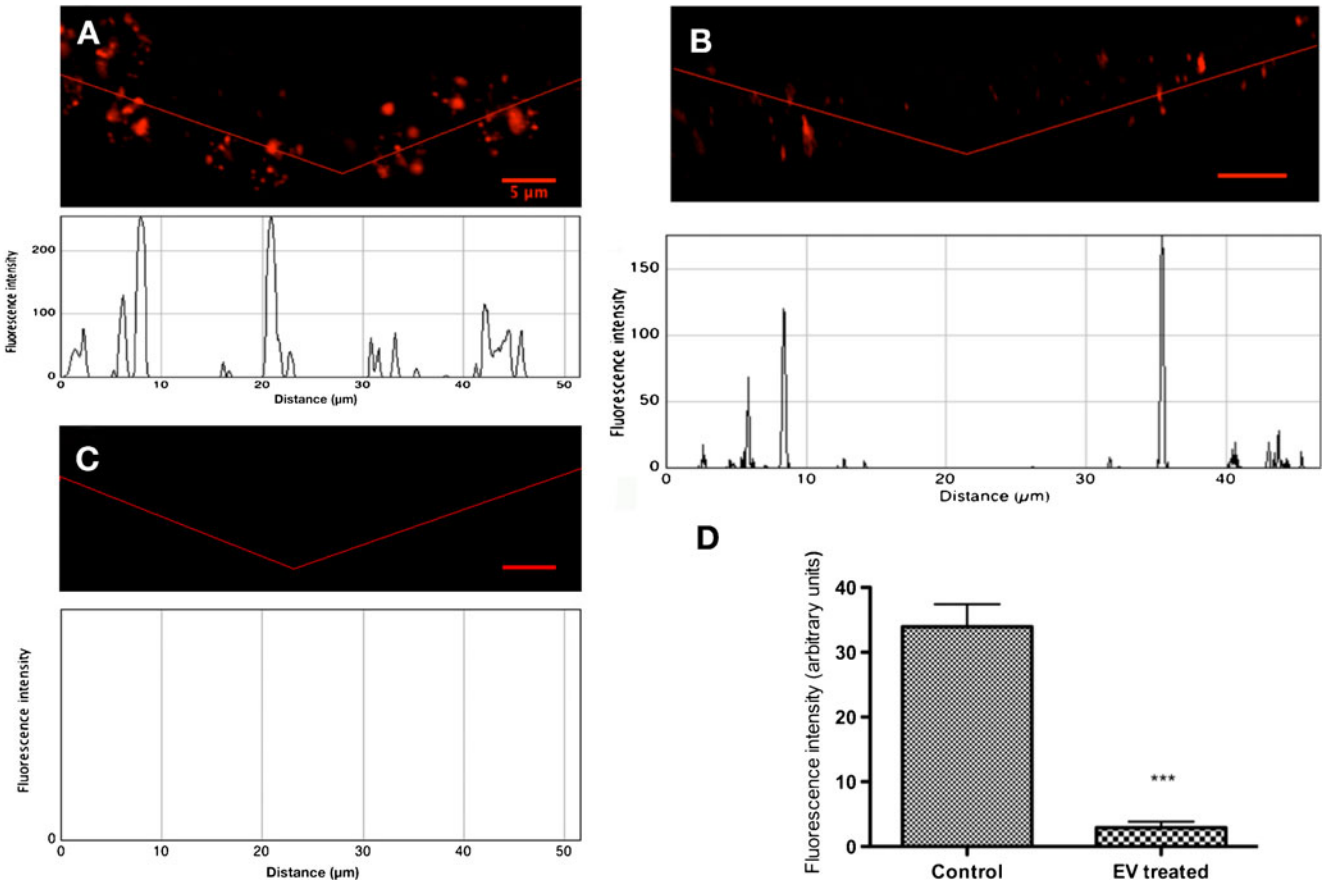

Fig. 4 ERβ1 immunofluorescence profiling in control and EV-treated mouse OSE. *Scale bar*=5 μm. **a** ERβ1 expression in control mouse. Profile shown below image. **b** EV-treated mouse OSE showing a large reduction in immunofluorescence. Profile shown below image. **c** Negative IgG isotype control showing no detectable immunoreactivity. Profile shown below image. **d** Mean fluorescence intensity scores from control and EV-treated mouse OSE (75 scans/group) were used to quantify ERβ and showed that EV treatment led to 11-fold reduction in ERβ1 expression ($p<0.0001$)

The present study used triple label immunofluorescence with high-resolution confocal imaging to optimally define ERα and ERβ1 protein expression patterns spatially in normal and estradiol-exposed OSE from older mice. Combining ERα/β (dual label) immunofluorescence emission profiles delineated sites of ER co-localization within individual OSE cells, and provided information on ER not previously reported with light microscopic evaluation, or with single label immunofluorescence. This work therefore extends existing knowledge of normal ER protein expression patterns in OSE [48, 49].

We found light microscopy did not optimally delineate nuclear from cytoplasmic expression, particularly with the ERβ1 isoform. Examination of ERα and ERβ1 with dual label technique generated measurable two-channel immunofluorescence profiles, and showed that although the two receptors visually colocalized in OSE cells, such "co-localization" was often the result of the two isoforms being separated by a very small distance. Since the optical (Z) slice for confocal imaging was <2 micron (1.8 μm), it may be inferred that when both ER isoforms were aligned in the same plane relative to the *z*-axis, and peak immunofluorescence emission produced by both ER within the OSE cell likewise aligned, ERα/β heterodimers had formed within ERβ clusters. However, in cells where peak ERα/β fluorescence emissions were separated by a greater distance (>2.0 micron), dynamic shuttling of the receptors to and from the nucleus into stochastically advantageous positions to facilitate heterodimer assembly may instead be occurring.

Continuous shuttling of mouse ERα has been shown to occur in cell culture [50], however studies are lacking on the nature of nuclear-cytoplasmic shuttling of ERβ in OSE. The variable nuclear and cytoplasmic expression of both ER isoforms that we observed from cell to cell in normal OSE, supports shuttling of ER between nucleus and cytoplasm. It is interesting that ERα/β co-expression appeared more common in cuboidal than columnar OSE, since columnar OSE is proposed to phenotypically resemble Müllerian duct-derived epithelia, potentially metaplastic and more prone to oncogenesis [51].

It is conceivable that translocation patterns of ERβ1 influence the formation of ERα/β heterodimers (known to modulate transcriptional activity of ERα) [52], possibly mediating ERα's proliferative influence in OSE [53]. Changes to sub-cellular expression and distribution of ER subtype are reported for breast cancer [54, 55] and have diagnostic and prognostic significance. For example, cytoplasmic expression of ERβ2 is associated with poor overall survival from breast cancer, whereas cytoplasmic expression of ERβ1 is not [54]. Additionally, heterodimers formed between ERβ1 and ERβ variants, β4 and β5 (a relationship that depends on the availability of ERβ1), may positively or negatively regulate ERβ1 activity in OSE and serve other functions, as yet unknown.

Further study of ER using the methods described here will extend knowledge of the *in vivo* distribution of ER subtypes and heterodimer formation in OSE, while allowing simultaneous quantitation of ER protein. This method could be of significant value to assess changes to ER that may predispose to ovarian epithelial cancer.

Acknowledgments The authors wish to thank Allan Herbison (Centre for Neuroendocrinology) and Maree Gould (Androgen Research group) in the Departments of Physiology and Anatomy and Structural Biology, University of Otago, for their kind donation of ERKO mouse tissue. We would also like to acknowledge the assistance of Mr. Robbie McPhee (graphics), Ms. Vicki Livingstone (statistical advice), and Mr. Andrew Mc Naughton (advice on confocal microscopic imaging).

Conflict of interest statement None declared.

References

1. Rodriguez C, Patel AV, Calle EE, Jacob EJ, Thun MJ (2001) Estrogen replacement therapy and ovarian cancer mortality in a large prospective study of US women. JAMA 285(11):1460–1465
2. Lacey JV Jr, Mink PJ, Lubin JH, Sherman ME, Troisi R, Hartge P et al (2002) Menopausal hormone replacement therapy and risk of ovarian cancer. JAMA 288(3):334–341
3. Lacey JV Jr, Brinton LA, Leitzmann MF, Mouw T, Hollenbeck A, Schatzkin A et al (2006) Menopausal hormone therapy and ovarian cancer risk in the National Institutes of Health-AARP Diet and Health Study Cohort. J Natl Cancer Inst 98(19):1397–1405
4. Riman T, Dickman PW, Nilsson S, Correia N, Nordlinder H, Magnusson CM et al (2002) Hormone replacement therapy and the risk of invasive epithelial ovarian cancer in Swedish women. J Natl Cancer Inst 94(7):497–504
5. Folsom AR, Anderson JP, Ross JA (2004) Estrogen replacement therapy and ovarian cancer. Epidemiology 15(1):100–104
6. Mills PK, Riordan DG, Cress RD (2004) Epithelial ovarian cancer risk by invasiveness and cell type in the Central Valley of California. Gynecol Oncol 95(1):215–225
7. Moorman PG, Schildkraut JM, Calingaert B, Halabi S, Berchuck A (2005) Menopausal hormones and risk of ovarian cancer. Am J Obstet Gynecol 193(1):76–82
8. Pearce CL, Chung K, Pike MC, Wu AH (2009) Increased ovarian cancer risk associated with menopausal estrogen therapy is reduced by adding a progestin. Cancer 115(3):531–539
9. Laviolette LA, Garson K, Macdonald EA, Senterman MK, Courville K, Crane CA et al (2010) 17beta-estradiol accelerates tumor onset and decreases survival in a transgenic mouse model of ovarian cancer. Endocrinology 151(3):929–938
10. Mangelsdorf DJ, Thummel C, Beato M, Herrlich P, Schutz G, Umesono K et al (1995) The nuclear receptor superfamily: the second decade. Cell 83(6):835–839
11. Green S, Walter P, Kumar V, Krust A, Bornert JM, Argos P et al (1986) Human oestrogen receptor cDNA: sequence, expression and homology to v-erb-A. Nature 320(6058):134–139
12. White R, Lees JA, Needham M, Ham J, Parker M (1987) Structural organization and expression of the mouse estrogen receptor. Mol Endocrinol 1(10):735–744
13. Kuiper GG, Carlsson B, Grandien K, Enmark E, Haggblad J, Nilsson S et al (1997) Comparison of the ligand binding specificity and transcript tissue distribution of estrogen receptors alpha and beta. Endocrinology 138(3):863–870
14. Mosselman S, Polman J, Dijkema R (1996) ER beta: identification and characterization of a novel human estrogen receptor. FEBS Lett 392(1):49–53
15. Tremblay GB, Tremblay A, Copeland NG, Gilbert DJ, Jenkins NA, Labrie F et al (1997) Cloning, chromosomal localization, and functional analysis of the murine estrogen receptor beta. Mol Endocrinol 11(3):353–365
16. Couse JF, Hewitt SC, Korach KS (2006) Steroid receptors in the ovary and uterus. In: Neill JD (ed) Knobil and Neill's Physiology of Reproduction. Third Edition.ed. Elsevier Academic Press, London, pp 593–678
17. Cowley SM, Hoare S, Mosselman S, Parker MG (1997) Estrogen receptors alpha and beta form heterodimers on DNA. J Biol Chem 272(32):19858–19862
18. Pace P, Taylor J, Suntharalingam S, Coombes RC, Ali S (1997) Human estrogen receptor beta binds DNA in a manner similar to and dimerizes with estrogen receptor alpha. J Biol Chem 272 (41):25832–25838
19. Tremblay GB, Tremblay A, Labrie F, Giguere V (1999) Dominant activity of activation function 1 (AF-1) and differential stoichiometric requirements for AF-1 and -2 in the estrogen receptor alpha–beta heterodimeric complex. Mol Cell Biol 19(3):1919–1927
20. Li X, Huang J, Yi P, Bambara RA, Hilf R, Muyan M (2004) Single-chain estrogen receptors (ERs) reveal that the ERalpha/beta heterodimer emulates functions of the ERalpha dimer in genomic estrogen signaling pathways. Mol Cell Biol 24(17):7681–7694
21. Leung YK, Mak P, Hassan S, Ho SM (2006) Estrogen receptor (ER)-beta isoforms: a key to understanding ER-beta signaling. Proc Natl Acad Sci U S A 103(35):13162–13167
22. Lubahn DB, Moyer JS, Golding TS, Couse JF, Korach KS, Smithies O (1993) Alteration of reproductive function but not prenatal sexual development after insertional disruption of the mouse estrogen receptor gene. Proc Natl Acad Sci U S A 90(23):11162–11166
23. Krege JH, Hodgin JB, Couse JF, Enmark E, Warner M, Mahler JF et al (1998) Generation and reproductive phenotypes of mice lacking estrogen receptor beta. Proc Natl Acad Sci U S A 95 (26):15677–15682
24. Lazennec G (2006) Estrogen receptor beta, a possible tumor suppressor involved in ovarian carcinogenesis. Cancer Lett 231 (2):151–157
25. Paruthiyil S, Parmar H, Kerekatte V, Cunha GR, Firestone GL, Leitman DC (2004) Estrogen receptor beta inhibits human breast cancer cell proliferation and tumor formation by causing a G2 cell cycle arrest. Cancer Res 64(1):423–428
26. Brandenberger AW, Tee MK, Jaffe RB (1998) Estrogen receptor alpha (ER-alpha) and beta (ER-beta) mRNAs in normal ovary,

ovarian serous cystadenocarcinoma and ovarian cancer cell lines: down-regulation of ER-beta in neoplastic tissues. J Clin Endocrinol Metab 83(3):1025–1028
27. Chan KK, Wei N, Liu SS, Xiao-Yun L, Cheung AN, Ngan HY (2008) Estrogen receptor subtypes in ovarian cancer: a clinical correlation. Obstet Gynecol 111(1):144–151
28. Bonkhoff H, Fixemer T, Hunsicker I, Remberger K (1999) Estrogen receptor expression in prostate cancer and premalignant prostatic lesions. Am J Pathol 155(2):641–647
29. Jakimiuk AJ, Weitsman SR, Yen HW, Bogusiewicz M, Magoffin DA (2002) Estrogen receptor alpha and beta expression in theca and granulosa cells from women with polycystic ovary syndrome. J Clin Endocrinol Metab 87(12):5532–5538
30. Mazouni C, Bonnier B, Goubar A, Romain S, Martin P (2010) Is quantitative oestrogen receptor expression useful in the evaluation of the clinical prognosis? Analysis of a homogeneous series of 797 patients with prospective determination of the ER status using simultaneous EIA and IHC. Eur J Cancer 46 (15):2716–2725
31. Liebelt AG, Sass B, Lombard LS (1987) Mouse ovarian tumors—a review including classification and induction of neoplastic lesions and description of several previously unreported types. J Exp Pathol 3(2):115–145
32. Tillmann T, Kamino K, Mohr U (2000) Incidence and spectrum of spontaneous neoplasms in male and female CBA/J mice. Exp Toxicol Pathol 52(3):221–225
33. Alison RH, Morgan KT (1987) Ovarian neoplasms in F344 rats and B6C3F1 mice. Environ Health Perspect 73:91–106
34. Moore CM, Hubbard GB, Leland MM, Dunn BG, Best RG (2003) Spontaneous ovarian tumors in twelve baboons: a review of ovarian neoplasms in non-human primates. J Med Primatol 32(1):48–56
35. Kaspareit J, Friderichs-Gromoll S, Buse E, Habermann G (2007) Spontaneous neoplasms observed in cynomolgus monkeys (Macaca fascicularis) during a 15-year period. Exp Toxicol Pathol 59(3–4):163–169
36. MacLachlan NJ (1987) Ovarian disorders in domestic animals. Environ Health Perspect 73:27–33
37. Jemal A, Murray T, Ward E, Samuels A, Tiwari RC, Ghafoor A et al (2005) Cancer statistics. CA Cancer J Clin 55(1):10–30
38. Wise PM (1982) Alterations in proestrous LH, FSH, and prolactin surges in middle-aged rats. Proc Soc Exp Biol Med 169(3):348–354
39. Wise PM, Smith MJ, Dubal DB, Wilson ME, Krajnak KM, Rosewell KL (1999) Neuroendocrine influences and repercussions of the menopause. Endocr Rev 20(3):243–248
40. Wise PM, Smith MJ, Dubal DB, Wilson ME, Rau SW, Cashion AB et al (2002) Neuroendocrine modulation and repercussions of female reproductive aging. Recent Prog Horm Res 57:235–256
41. Prior JC (1998) Perimenopause: the complex endocrinology of the menopausal transition. Endocr Rev 19(4):397–428
42. Prior JC (2005) Ovarian aging and the perimenopausal transition: the paradox of endogenous ovarian hyperstimulation. Endocrine 26(3):297–300
43. Hiroi H, Inoue S, Watanabe T, Goto W, Orimo A, Momoeda M et al (1999) Differential immunolocalization of estrogen receptor alpha and beta in rat ovary and uterus. J Mol Endocrinol 22 (1):37–44
44. Chu S, Fuller PJ (1997) Identification of a splice variant of the rat estrogen receptor beta gene. Mol Cell Endocrinol 132(1–2):195–199
45. Barros RP, Machado UF, Warner M, Gustafsson JA (2006) Muscle GLUT4 regulation by estrogen receptors ERβ and ERα. Proc Natl Acad Sci U S A 103(5):1605–1608
46. Gould ML, Hurst PR, Nicholson HD (2007) The effects of oestrogen receptors alpha and beta on testicular cell number and steroidogenesis in mice. Reproduction 134(2):271–279
47. Wang C, Prossnitz ER, Roy SK (2007) Expression of G protein-coupled receptor 30 in the hamster ovary: differential regulation by gonadotropins and steroid hormones. Endocrinology 148 (10):4853–4864
48. Hishikawa Y, Damavandi E, Izumi S, Koji T (2003) Molecular histochemical analysis of estrogen receptor alpha and beta expressions in the mouse ovary: in situ hybridization and Southwestern histochemistry. Med Electron Microsc 36(2):67–73
49. Symonds D, Tomic D, Borgeest C, McGee E, Flaws JA (2003) Smad 3 regulates proliferation of the mouse ovarian surface epithelium. Anat Rec A Discov Mol Cell Evol Biol 273(2):681–686
50. Dauvois S, White R, Parker MG (1993) The antiestrogen ICI 182780 disrupts estrogen receptor nucleocytoplasmic shuttling. J Cell Sci 106(Pt 4):1377–1388
51. Auersperg N, Wong AS, Choi KC, Kang SK, Leung PC (2001) Ovarian surface epithelium: biology, endocrinology, and pathology. Endocr Rev 22(2):255–288
52. Hall JM, McDonnell DP (1999) The estrogen receptor beta-isoform (ERbeta) of the human estrogen receptor modulates ERalpha transcriptional activity and is a key regulator of the cellular response to estrogens and antiestrogens. Endocrinology 140(12):5566–5578
53. Bai W, Oliveros-Saunders B, Wang Q, Acevedo-Duncan ME, Nicosia SV (2000) Estrogen stimulation of ovarian surface epithelial cell proliferation. In Vitro Cell Dev Biol Anim 36 (10):657–666
54. Shaaban AM, Green AR, Karthik S, Alizadeh Y, Hughes TA, Harkins L et al (2008) Nuclear and cytoplasmic expression of ERbeta1, ERbeta2, and ERbeta5 identifies distinct prognostic outcome for breast cancer patients. Clin Cancer Res 14(16):5228–5235
55. Lazennec G, Bresson D, Lucas A, Chauveau C, Vignon F (2001) ER beta inhibits proliferation and invasion of breast cancer cells. Endocrinology 142(9):4120–4130